

# Spin distribution following minor mergers and the effect of spin on the detection range for low-mass-ratio inspirals

Ilya Mandel

*Theoretical Astrophysics, California Institute of Technology, Pasadena, California 91125*

ilya@caltech.edu

## ABSTRACT

We compute the probability distribution for the spin of a black hole following a series of minor mergers with isotropically distributed, non-spinning, inspiraling compact objects. By solving the Fokker-Planck equation governing this stochastic process, we obtain accurate analytical fits for the evolution of the mean and standard deviation of the spin distribution in several parameter regimes. We complement these analytical fits with numerical Monte-Carlo simulations in situations when the Fokker-Planck analysis is not applicable. We find that a  $\sim 150 M_\odot$  intermediate-mass black hole that gained half of its mass through minor mergers with neutron stars will have dimensionless spin parameter  $\chi = a/M \sim 0.2 \pm 0.08$ . We estimate the effect of the spin of the central black hole on the detection range for intermediate-mass-ratio inspiral (IMRI) detections by Advanced LIGO and extreme-mass-ratio inspiral (EMRI) detections by LISA. We find that for realistic black hole spins, the inclination-averaged Advanced-LIGO IMRI detection range may be increased by up to 10% relative to the range for IMRIs into non-spinning intermediate-mass black holes. For LISA, we find that the detection range for EMRIs into  $10^5 M_\odot$  massive black holes (MBHs) is not significantly affected by MBH spin, the range for EMRIs into  $10^6 M_\odot$  MBHs is affected at the  $\lesssim 10\%$  level, and EMRIs into maximally spinning  $10^7 M_\odot$  MBHs are detectable to a distance  $\sim 25$  times greater than EMRIs into non-spinning black holes. The resulting bias in favor of detecting EMRIs into rapidly spinning MBHs will play a role when extracting the MBH spin distribution from EMRI statistics.

*Subject headings:* black hole physics — gravitational waves

## 1. Introduction

A growing body of evidence from observations, numerical simulations, and comparisons between the two, suggests the existence of a population of intermediate-mass black holes with

masses in the  $M \sim 10^2 - 10^4 M_\odot$  range (e.g., (Miller & Colbert 2004) and references therein). These intermediate-mass black holes may capture compact objects (stellar-mass black holes or neutrons stars) and merge with them (Taniguchi et al. 2000; Miller & Hamilton 2002a,b; Mouri & Taniguchi 2002a,b; Gültekin, Miller, & Hamilton 2004, 2006; O’Leary et al. 2006; Mandel et al. 2007). In addition to adding to the black-hole mass, the merging compact objects will also contribute their orbital angular momentum to the spin angular momentum of the central black hole, leading to the evolution of the black-hole spin through a sequence of such minor mergers.

We might expect the typical spin of a black hole to be low if a significant fraction of its mass has been added via minor mergers with compact objects whose angular momentum at plunge is distributed isotropically. The angular momentum imparted to the black hole of mass  $M$  by a compact object of mass  $m$  is  $L_{\text{obj}} \propto mM$ . (We include only the orbital angular momentum, not the spin angular momentum of the compact object, since the latter is lower than the former by a factor of order  $m/M$ , which we assume to be small for minor mergers.) This causes the dimensionless spin parameter of the hole  $\chi \equiv S_1/M^2 = a/M$  to change by  $\sim L_{\text{obj}}/M^2 \propto m/M$ . After  $N \sim M/m$  such mergers, necessary for the hole to grow to mass  $M$ , the typical dimensionless spin parameter of the hole will be  $\chi \propto (m/M)\sqrt{N} \sim \sqrt{m/M}$ .

As discussed by Miller (2002) and Hughes & Blandford (2004), the angular momenta of black holes that grow through minor mergers undergo a damped random walk. The damping comes about because retrograde orbits, which subtract angular momentum from a black hole, plunge from a last stable orbit (LSO) at a higher radius than prograde orbits, so more angular momentum is subtracted following retrograde inspirals than is added following prograde ones.

In this paper, we make an analytical approximation to the spin change induced by a minor merger and solve the Fokker-Planck equation to obtain the evolution of the spin probability distribution (Hughes & Blandford 2004). (We use a simpler one-dimensional version of the Fokker-Planck equation than Hughes & Blandford (2004), since we are interested only in the evolution of the magnitude of the spin, not its direction.) We find that for black holes with  $\chi \gg \sqrt{m/M}$ , the spin  $\chi$  evolves proportionally to  $M^{-2.63}$  as the mass grows via minor mergers (rather than  $M^{-2}$ , which would be the case without damping). We determine the asymptotic values of the expected mean of the spin distribution and its standard deviation in the limit of infinitely many minor mergers:  $\bar{\chi} \rightarrow \sqrt{1.5m/M}$  and  $\sigma \rightarrow \sqrt{0.7m/M}$ . We also describe the evolution of the spin distribution in other parameter regimes, e.g., when  $\sqrt{m/M} \gg \chi \gg m/M$ .

Our Fokker-Planck analysis fails when the mass ratio  $m/M$  is not sufficiently low, so for those cases we resort to Monte-Carlo numerical simulations. We find that if the mass

of the central black hole grows from  $M = 5m$  to  $M = 10m$  by capturing five objects of equal mass  $m$ , the mean spin of the resulting black hole is  $\bar{\chi} \approx 0.5$ , nearly independent of its initial spin (Miller (2002) obtained similar results). However, if the central black hole grows from  $M = 50m$  to  $M = 100m$  (e.g., a  $M = 70 M_\odot$  black hole growing to  $M = 140 M_\odot$  by capturing fifty  $m = 1.4 M_\odot$  neutron stars), its resulting spin is rather low,  $\chi \sim 0.2 \pm 0.08$ .

The combination of the spin of the central black hole and the inclination of the inspiraling object’s orbit can have a significant effect on the gravitational-wave signal from a low-mass-ratio inspiral. We compute the increase in the Advanced-LIGO detection range for intermediate-mass-ratio inspirals (IMRIs) due to the spin of the central black hole. We find that the detection range, averaged over orbital inclinations, may increase by  $\sim 3 - 10\%$  relative to the range for inspirals into non-spinning black holes for the expected values of black hole mass and spin. We provide an approximate expression for the dependence of the Advanced-LIGO IMRI detection range on spin [see Eq. (24)]. We also compute the change in the LISA extreme-mass-ratio-inspiral (EMRI) detection range due to the spin of the massive black hole. We find that the range for inspirals into  $M = 10^5 M_\odot$  black holes is nearly independent of their spin, because the frequency at the last stable orbit (LSO) is away from the minimum of the LISA noise curve. On the other hand, the inclination-averaged detection range for IMRIs into rapidly spinning  $M = 10^7 M_\odot$  black holes is  $\sim 25$  times greater than into non-spinning ones. The detection volumes are proportional to the cube of the range. This will create a bias in favor of detecting inspirals into rapidly spinning black holes, which in turn will have consequences for the extraction of massive-black-hole spin function from LISA EMRI statistics.

The paper is organized as follows. In Sec. 2, we provide the background for our calculation of the spin evolution via minor mergers. In Sec. 3, we describe analytical solutions of the Fokker-Planck equation for spin evolution. In Sec. 4, we describe Markov-Chain numerical simulations of spin evolution. In Sec. 5, we evaluate the dependence of the detection ranges for low-mass-ratio inspirals averaged over orbital inclination angles on the spin of the massive body, in the context of both Advanced LIGO and LISA.

## 2. Spin evolution

We assume that the distribution of the orbital inclination angle  $\iota$  relative to the central black hole’s spin is isotropic at capture. Here  $\iota$  is defined via

$$\cos \iota = \frac{L_z}{\sqrt{L_z^2 + Q}}, \quad (1)$$

$L_z$  is the object’s orbital angular momentum in the direction of the black hole’s spin, and  $Q$  is the Carter constant. We further assume that the inclination angle  $\iota$  remains approximately constant over the inspiral (Hughes 2000), so the distribution of inclinations at the LSO is also isotropic,  $\text{Pr}(\cos \iota) = 1/2$ .

In the low-mass-ratio limit, the amount of angular momentum radiated in gravitational waves during the plunge and ringdown is smaller by a factor of  $\sim m/M$  than the angular momentum at the LSO. Therefore, we assume that the merging object contributes its orbital angular momentum at the LSO to the angular momentum of the black hole. The spin of the black hole after a minor merger,  $\chi'$ , is related to the original spin  $\chi$  via

$$\chi' \approx \frac{1}{(M+m)^2} \sqrt{(\chi M^2 + L_z)^2 + Q}, \quad (2)$$

where  $m$  is the mass of the small object,  $M$  is the mass of the hole, and we assume  $m \ll M$ .

The constants of motion  $L_z$  and  $Q$  at the LSO can be obtained as a function of  $\iota$  by demanding that the potential  $R$  and its first and second derivatives in  $r$  are zero at the LSO (see Chapter 33 of (Misner, Thorne, & Wheeler 1973)):

$$\begin{aligned} R &= [E(r^2 + \chi^2 M^2) - L_z \chi M]^2 - (r^2 - 2Mr + \chi^2 M^2) [m^2 r^2 + (L_z - \chi M E)^2 + Q], \\ R &= 0, \quad \frac{dR}{dr} = 0, \quad \frac{d^2 R}{dr^2} = 0 \quad \text{at LSO.} \end{aligned} \quad (3)$$

It is possible to make analytic approximations to the values of  $L_z$  and  $Q$  at the LSO based on appropriately averaging the analytically known constants of motion at the LSO for prograde and retrograde equatorial orbits (cf. Eq. (9) of (Hughes & Blandford 2004)). In particular, for  $\chi \ll 1$ , the plunging object’s dimensionless “total angular momentum” is given by

$$\hat{L} = \frac{\sqrt{L_z^2 + Q}}{Mm} \approx Mm\sqrt{12} \left[ 1 - \frac{1}{2} \left( \frac{2}{3} \right)^{3/2} \chi \cos \iota \right], \quad (4)$$

where we correct a mistake in Eq. (4) of (Miller 2002). Then  $L_z$  and  $Q$  follow from Eq. (1):

$$L_z = \cos \iota \sqrt{L_z^2 + Q}; \quad Q = \sin \iota \sqrt{L_z^2 + Q}. \quad (5)$$

### 3. Fokker-Planck equation for spin evolution

The black-hole spin evolution is a stochastic process. The probability distribution function of a stochastic process, however, can be described the deterministic Fokker-Planck

equation:

$$\frac{\partial}{\partial t} f(x, t) = -\frac{\partial}{\partial x} [\mu(x, t) f(x, t)] + \frac{1}{2} \frac{\partial^2}{\partial x^2} [\sigma^2(x, t) f(x, t)], \quad (6)$$

where  $\mu = \langle dx \rangle / dt$  is the mean drift and  $\sigma^2 = \langle (dx)^2 \rangle / dt$  is the stochastic variance. In this Section, we derive approximate analytical solutions to the Fokker-Planck equation in several interesting parameter regimes.

For simplicity, assume that all merging objects have the same mass  $m$ . We parametrize the mass of the black hole by a dimensionless “time” parameter  $t = M/m$ . The change in the spin  $\chi$  after a merger follows from Eq. (2):

$$d\chi = \frac{1}{(t+1)^2} \sqrt{\chi^2 t^4 + \hat{L}^2 t^2 + 2\chi \hat{L} t^3 \cos \iota} - \chi. \quad (7)$$

We can compute  $\hat{L}$  at plunge as a function of  $\chi$  and  $\cos \iota$  by solving Eqs. (3), then substituting the result into Eq. (7) to obtain  $d\chi$  as a function of  $t$ ,  $\chi$ , and  $\cos \iota$ . Although this process is simple in principle, such a numerical computation makes it impossible to obtain analytic expressions for  $\langle d\chi \rangle$  and  $\langle (d\chi)^2 \rangle$ , which are necessary if we wish to solve the Fokker-Planck equation. (Here, brackets denote averaging over  $\cos \iota$ .)

We could, of course, try to obtain empirical analytic fits to the numerical solutions for  $\langle d\chi \rangle$  and  $\langle (d\chi)^2 \rangle$ , but it turns out that there is a simpler approach. The approximate formula for  $\hat{L}$  given in Eq. (4) is valid only when  $\chi \ll 1$ ; when  $\chi \sim 1$ , Eq. (4) overestimates  $\hat{L}$  by as much as 40%. Remarkably, however, using this incorrect approximation for  $\hat{L}$  in Eq. (7) generally yields very accurate expressions for  $\langle d\chi \rangle$  for a wide range of  $\chi$ . So long as  $\chi t \gg 1$  (i.e.,  $\chi \gg m/M$ ), an expansion of Eq. (7) to the first order in  $1/(\chi t)$  yields the following simple analytic expression for the mean drift in  $\chi$ :

$$\mu(\chi, t) = \frac{\langle d\chi \rangle}{dt} = \frac{\chi}{t} \left( -2 - \frac{4\sqrt{2}}{9} \right) + \frac{4}{\chi t^2}. \quad (8)$$

This expression is accurate to about 1% for all values of  $\chi$  so long as  $\chi t \gtrsim 10$ . Similarly, the analytic expression for the stochastic variance of the spin is

$$\sigma^2(\chi, t) = \frac{\langle (d\chi)^2 \rangle}{dt} = \frac{4}{t^2} \left( 1 + \frac{4\sqrt{2}\chi^2}{9} - \chi^2 \right). \quad (9)$$

This expression underestimates the variance by  $\gtrsim 10\%$  for very high spins, but is generally accurate to a few percent for lower spins which are expected as a consequence of minor mergers in the Advanced LIGO setting.

We can now substitute Eqs. (8) and (9) into the Fokker-Planck equation for the probability evolution (6) to obtain

$$\begin{aligned} \frac{\partial}{\partial t} f(\chi, t) &= -\frac{\partial}{\partial \chi} \left[ \frac{\chi}{t} \left( -2 - \frac{4\sqrt{2}}{9} + \frac{4}{\chi^2 t} \right) f(\chi, t) \right] \\ &+ \frac{1}{2} \frac{\partial^2}{\partial \chi^2} \left[ \frac{4}{t^2} \left( 1 + \frac{4\sqrt{2}\chi^2}{9} - \chi^2 \right) f(\chi, t) \right]. \end{aligned} \quad (10)$$

This is a one-dimensional equation unlike the three-dimensional equation derived in (Hughes & Blandford 2004), since we choose to focus on the evolution of the magnitude of the spin, not its direction. Still, this is a rather complicated equation that does not easily separate. Fortunately, for many applications it is not necessary to solve the complete equation.

Equation (10) was derived under the assumption  $\chi t \gg 1$ . If we further assume that  $\chi^2 t \gg 1$  (i.e.,  $\chi \gg \sqrt{m/M}$ ), then the mean spin evolution is dominated by

$$\frac{d\bar{\chi}}{dt} \approx a \frac{\bar{\chi}}{t}, \quad (11)$$

where  $a \equiv -2 - 4\sqrt{2}/9 \approx -2.63$ . (This result can also be obtained directly from Eq. (8).) Thus, the mean spin evolves according to

$$\bar{\chi} \approx \bar{\chi}_0 \left( \frac{t}{t_0} \right)^a \approx \bar{\chi}_0 \left( \frac{M_0}{M} \right)^{2.63} \quad (12)$$

(compare with Eq. (26) of (Hughes & Blandford 2004), where the exponent is approximated by 2.4).

If the assumption  $\chi^2 t \gg 1$  is not satisfied, and instead  $\chi^2 t \ll 1$ , but  $\chi t \gg 1$  so that Eq. (10) still holds, the evolution of the probability function may be approximated as

$$\frac{\partial f(t, \chi)}{\partial t} = -\frac{\partial}{\partial \chi} \left( \frac{4f(t, \chi)}{\chi t^2} \right) + \frac{1}{2} \frac{\partial^2}{\partial \chi^2} \left( \frac{4f(t, \chi)}{t^2} \right). \quad (13)$$

This equation can be solved by separation of variables:  $f(t, \chi) = T(t)X(\chi)$ , where the solution for  $T$  is  $T(t) = \exp(-k/t)$ ,  $X$  is the solution to

$$2\chi^2 X'' - 4\chi X' + 4X - k\chi^2 X = 0, \quad (14)$$

and  $k$  is a constant. The mean spin grows roughly as

$$\bar{\chi} \sim \sqrt{\frac{2}{t_0} - \frac{2}{t}}, \quad (15)$$

so after  $t \gtrsim 2t_0$  (i.e., after the black hole captures half its mass via minor mergers),  $\chi^2 t \gtrsim 1$ .

The spin growth and spin decay terms in Eq. (10) cancel when the spin is approximately equal to

$$\bar{\chi} \rightarrow \sqrt{\frac{4}{-at}} \approx \sqrt{\frac{1.5}{t}}. \quad (16)$$

(Compare with Miller (2002), who estimated the mean spin to be  $\sqrt{2}\sqrt{(m/M)} = \sqrt{2/t}$  based on numerical simulations.)

We can estimate the second moment of the probability distribution by approximating the solution to Eq. (10) by a Gaussian (as suggested by Miller (2002)):

$$f(\chi, t) = \frac{1}{\sqrt{2\pi}\sigma} \exp \left[ -\frac{(\chi - \bar{\chi}(t))^2}{2\sigma^2(t)} \right]. \quad (17)$$

(A Gaussian turns out to be a good approximation except at small  $\bar{\chi}$ , when the tails at  $\chi > \bar{\chi}$  are larger than those at  $\chi < \bar{\chi}$ .) Substituting this Gaussian into Eq. (10), keeping only the lowest-order terms in  $t\chi$ , and setting  $\chi = \bar{\chi}$ , we obtain

$$-\frac{1}{\sigma} \frac{d\sigma}{dt} = -\frac{a}{t} - \frac{2}{t^2\sigma^2}(1 + b\bar{\chi}^2), \quad (18)$$

where  $b \equiv 4\sqrt{2}/9 - 1$ . If  $\sigma^2 t \gg 1$ , then  $\sigma$  evolves in the same way as  $\bar{\chi}$  when  $\chi^2 t \gg 1$ :

$$\sigma \approx \sigma_0 \left( \frac{t}{t_0} \right)^a \approx \sigma_0 \left( \frac{M_0}{M} \right)^{2.63}. \quad (19)$$

What if  $\sigma^2 t \ll 1$ ? This might be the case of interest if, say, the initial spin of a black hole created during some process is known precisely, and we wish to estimate future spin evolution through minor mergers. In this case, the second term on the right-hand side of Eq. (18) dominates, and if  $\bar{\chi}$  is small or does not change significantly,  $\sigma$  grows according to

$$\sigma \approx \sqrt{4(1 + b\bar{\chi}^2) \left( \frac{1}{t_0} - \frac{1}{t} \right) + \sigma_0^2}. \quad (20)$$

In either case,  $\sigma$  asymptotes to the solution

$$\sigma \rightarrow \sqrt{\frac{2(1 + b\bar{\chi}^2)}{-at}}. \quad (21)$$

For large  $t$ ,  $\sigma \sim \sqrt{2/(-at)} \approx \sqrt{0.7/t}$ ; Miller (2002) estimated  $\sigma$  to be  $\sqrt{(m/M)}/\sqrt{2} = \sqrt{1/(2t)}$  based on numerical simulations.

Lastly, consider the case when  $\chi t \lesssim 1$ . In this case the orbital angular momentum of the plunging object is comparable to the spin angular momentum of the black hole, and Eq. (10) is incorrect, since it was derived under the assumption  $\chi t \gg 1$ . If the black hole is initially non-spinning or has spin  $\chi \lesssim 1/t$ , however, a single minor merger will bring its spin to  $\chi \sim \sqrt{12}/t$  according to Eq. (7). This case can be treated with a Monte-Carlo numerical simulation as described in the next section.

#### 4. Spin evolution via Monte Carlo simulations

We have carried out Monte Carlo simulations of spin evolution through minor mergers in order to confirm the analytical estimates presented above, based on the approximate Fokker-Planck equation. Our simulations also allow us to access the small- $t$  regime where the Fokker-Planck approach is not valid, but where our physical approximations for low-mass-ratio inspirals still hold. Since these simulations were performed numerically, there was no need to make analytical approximations to  $d\chi$  following a merger; instead, we solved Eqs. (3) directly and obtained  $d\chi$  via Eq. (7).

In Figure 1 we plot the spin distribution of a black hole of mass  $t = M/m = 10$  that started out with either spin  $\chi = 0.1$  or  $\chi = 0.9$  at  $t = M/m = 5$  before growing via minor mergers. This corresponds, for example, to an intermediate-mass black hole that grows from  $M = 50 M_\odot$  to  $M = 100 M_\odot$  by capturing  $m = 10 M_\odot$  black holes. The distributions for both values of initial spin are roughly Gaussian, although with shorter-than-Gaussian tails (we plot the actual Monte-Carlo histogram for the  $\chi = 0.9$  case for comparison with a fitted Gaussian). We see that for these small values of  $t$ , the initial value of the spin is largely forgotten after the black hole captures half of its mass through minor mergers. The means of the spin at  $t = 10$  are  $\bar{\chi} = 0.49$  for the initially slowly-spinning hole and  $\bar{\chi} = 0.51$  for the initially rapidly-spinning hole. The standard deviations at  $t = 10$  are  $\sigma = 0.17$  for initial spin  $\chi = 0.1$  and  $\sigma = 0.18$  for initial spin  $\chi = 0.9$  (the initial standard deviations are zero in both cases, i.e., the initial spins are presumed to be precisely determined). These results agree with Fig. 1 of (Miller 2002). Because the values of  $t$  involved are so small, the Fokker-Planck equation (10) does not apply: at  $t = 5$ , the angular momentum of the inspiraling object at the LSO is comparable to or larger than the spin angular momentum of the black hole even for large initial black hole spins.

In Figure 2 we plot the spin distribution for a black hole of mass  $t = M/m = 100$  that started out at  $t = M/m = 50$  at either spin  $\chi = 0.1$  or  $\chi = 0.9$  before growing via minor mergers. This corresponds, for example, to an intermediate-mass black hole that grows from  $70 M_\odot$  to  $140 M_\odot$  by capturing  $M = 1.4 M_\odot$  neutron stars. The means of the



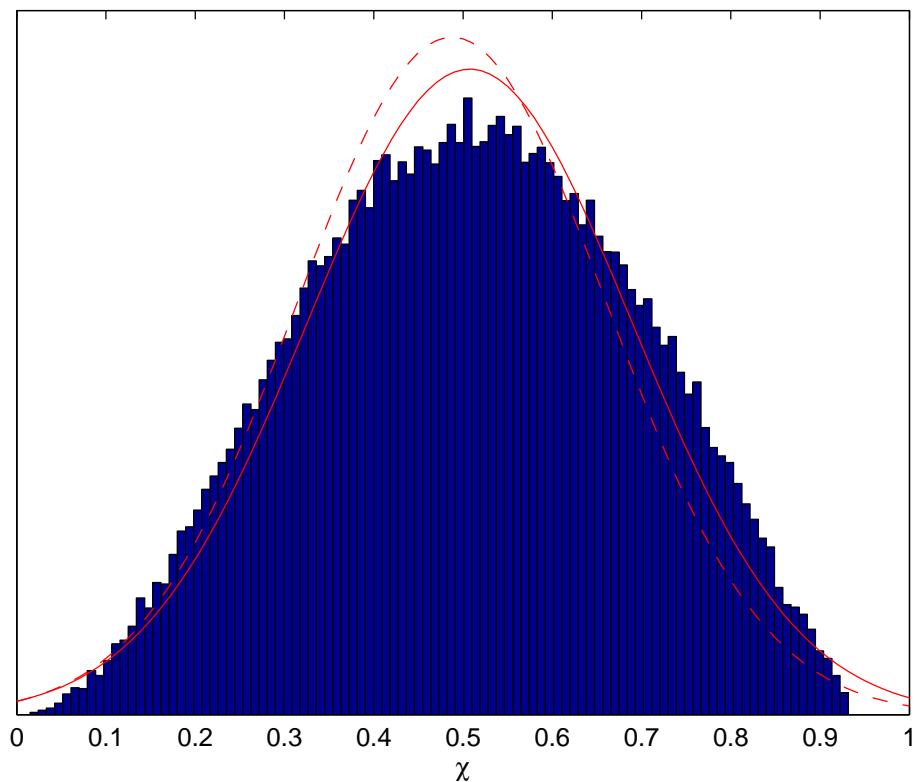


Fig. 1.— Monte-Carlo predictions for the black-hole spin distribution following black-hole growth via minor mergers from  $t = M/m = 5$  to  $t = M/m = 10$ . The histogram shows the spin distribution at  $t = 10$  for a black hole with initial spin  $\chi = 0.9$ , and the solid curve is a Gaussian fit to that distribution. The dashed curve is a Gaussian fit to the spin distribution at  $t = 10$  for a black hole that has initial spin  $\chi = 0.1$  at  $t = 5$ .

spin at  $t = 100$  are  $\bar{\chi} = 0.162$  for the initially slowly-spinning hole and  $\bar{\chi} = 0.233$  for the initially rapidly-spinning hole. The final spin in the initially rapidly-spinning case decreases as  $\bar{\chi} \sim \chi_0(t/t_0)^{-2}$ , rather than  $\bar{\chi} \sim \chi_0(t/t_0)^{-2.63}$  as predicted by Eq. (12). That is because the spin begins to approach the asymptotic value of  $\bar{\chi} \approx \sqrt{1.5/t} \approx 0.12$  as predicted by Eq. (16), and the rate of spin evolution decreases because  $\chi^2 t$  is no longer much greater than one. The initially slowly-spinning case does not quite satisfy  $\chi t \gg 1$ , so the Fokker-Planck analysis is suspect; however, Eq. (15), relevant since  $\chi^2 t < 1$  in this case, provides a roughly accurate estimate of spin growth. The standard deviations at  $t = 100$  are  $\sigma = 0.066$  for initial spin  $\chi = 0.1$  and  $\sigma = 0.084$  for initial spin  $\chi = 0.9$ ; the predicted asymptotic value of the standard deviation according to Eq. (21) is  $\sigma = 0.087$ . The mass ratios considered in this paragraph may be plausible for intermediate-mass-ratio inspirals into intermediate-mass black holes that would be detectable with Advanced LIGO (Mandel et al. 2007).

Finally, we perform a Monte-Carlo simulation of the evolution of a spin distribution from  $t = 1100$  to  $t = 1200$  where the starting mean spin is  $\bar{\chi} = 0.72$  and the starting standard deviation is  $\sigma = 0.016$ . In this case,  $\chi^2 t \gg 1$  holds throughout the evolution, so this example can be viewed as a test of our Fokker-Planck analysis. Based on Eq. (12), we expect the spin at  $t = 1200$  to decrease to  $\bar{\chi} = 0.57$ ; in fact, we find  $\bar{\chi}(t = 1200) = 0.58$ . Since  $\sigma^2 t \ll 1$ , we expect the standard deviation to grow via Eq. (20) to  $\sigma = 0.022$  at  $t = 1200$ ; in fact,  $\sigma(t = 1200) = 0.021$ .

The Fokker-Planck analysis should give excellent results in the regime of very large  $t$ , such as those corresponding to minor mergers of stellar-mass compact objects with  $\sim 10^6 M_\odot$  massive black holes in galactic centers. (The extreme-mass-ratio inspirals preceding such minor mergers are an interesting class of potential LISA sources (Amaro-Seoane et al. 2007).) On the other hand, if a large range of  $t$  must be covered, Monte-Carlo simulations become expensive. Thus, the Monte-Carlo numerical methods and Fokker-Planck analysis can be viewed as complementary techniques.

## 5. Effect of black-hole spin on detection ranges for low-mass-ratio inspirals

The frequency of the last stable orbit before plunge is strongly influenced by the black-hole spin and the orbital inclination. Prograde inspirals into rapidly spinning black holes will have much higher LSO frequencies than inspirals into non-spinning black holes or polar inspirals into spinning black holes of the same mass, while retrograde inspirals into rapidly spinning black holes will have lower LSO frequencies. For example, for a maximally spinning Kerr black hole, the frequency of the LSO of a retrograde equatorial inspiral is twice lower than for a polar orbit, while the LSO frequency of a prograde equatorial inspiral is six

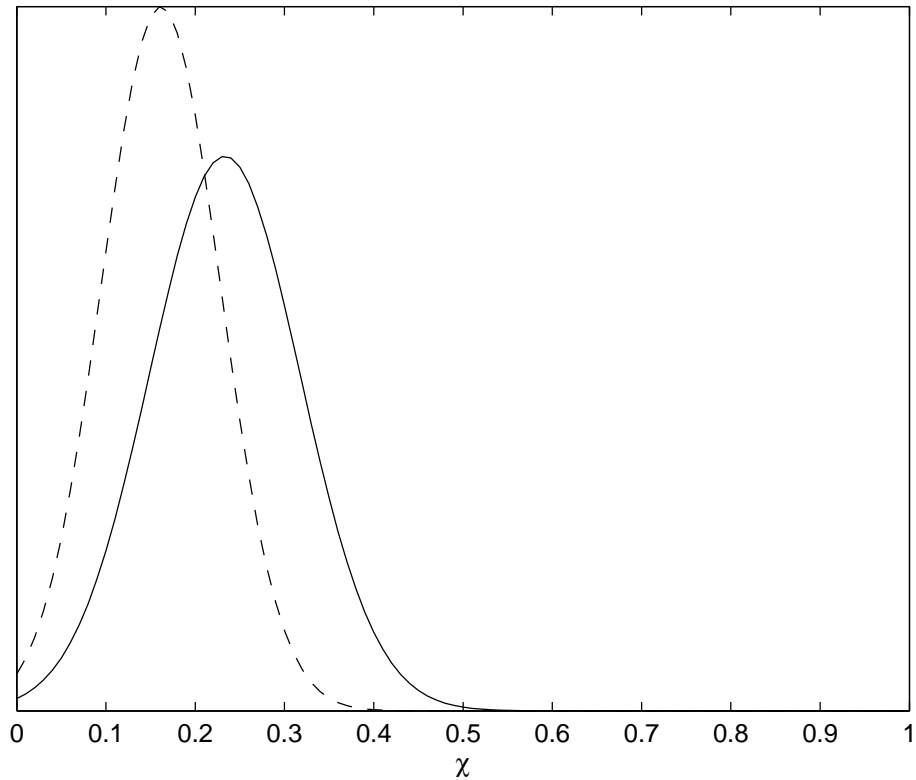


Fig. 2.— Monte-Carlo black-hole spin distribution following black hole growth via minor mergers from  $t = M/m = 50$  to  $t = M/m = 100$ . The spin distribution for a black hole with initial spin  $\chi = 0.9$  is shown with a solid curve, and one for initial spin  $\chi = 0.1$  is shown with a dashed curve.

times higher than for a polar orbit. Even for a more moderately spinning black hole with  $\chi = 0.4$ , there is almost a factor of two difference between LSO frequencies for prograde and retrograde inspirals.

The signal-to-noise ratio (SNR) for the detection of gravitational waves from inspirals depends on where the LSO frequency falls on the noise power spectral density curve of the detector. Although some inclination angles will increase SNR and others will decrease it, we might generally expect that average detection range for inspirals into spinning black holes will be higher than into non-spinning ones. (“Average” refers to averaging over the isotropically distributed orbital inclination angles of the inspiraling object.) This is because of the cubic dependence of the detection volume on detection range, which is proportional to SNR: if, say, 10% of all inspirals have their SNR boosted by a factor of three, these will be seen three times further and the detection volume for these kinds of inspirals will go up by a factor of 27, so the average volume in which detections can be made will increase by a factor of  $\sim 3$ , and the average detection range will grow by the cube root of 3.

Conversely, this average detection range increase can manifest itself as a bias in favor of detecting inspirals into rapidly spinning black holes rather than slowly spinning ones. Thus, a numerical estimate of the detection range increase due to black hole spin is useful for determining whether a high fraction of rapidly spinning black holes among detected inspirals is an indication of the prevalence of such black holes in the universe, or whether this is merely a selection effect.

We use the simple scaling

$$|\tilde{h}(f)^2| \propto f^{-7/3} \quad (22)$$

for the frequency-domain gravitational wave. The square of the signal-to-noise ratio  $\rho^2$  is proportional to

$$\rho^2 \propto \int_{f_{\min}}^{f_{\max}} \frac{|\tilde{h}(f)^2|}{S_n(f)} df \propto \int_{f_{\min}}^{f_{\max}} \frac{f^{-7/3}}{S_n(f)} df. \quad (23)$$

Here,  $S_n(f)$  is the noise power spectral density of the detector,  $f_{\max}$  is the frequency of gravitational waves from the last stable orbit, and  $f_{\min}$  is the low-frequency cutoff for the detector for Advanced LIGO, where  $f_{\min} = 10$  Hz, or the frequency of gravitational waves one year before plunge for LISA. We set  $f_{\max}$  equal to twice the orbital frequency at the LSO, which we obtain numerically as a function of the black-hole mass  $M$  and spin  $\chi$  and of the orbital inclination angle  $\cos \iota$  by solving Eq. (3).

The distance to which an event can be seen is proportional to SNR,  $\rho$ , so the detection volume is proportional to  $\rho^3$ . Therefore, we average  $\rho^3$ , computed via Eq. (23), over the different inclinations  $\cos \iota$  (uniformly distributed through the range  $[-1, 1]$ ) in order to

compute the expected increase in the detection volume for a given values of  $\chi$ , and then take the cube root to compute the increase in the average detection range.

We have computed detection ranges for Advanced LIGO using this method with the noise power spectral density  $S_n(|f|)$  taken from (Fritschel 2003). Fig. 3 shows our computed ratio between (i) the average Advanced-LIGO detection range for intermediate-mass-ratio inspirals into black holes of a given mass and spin and (ii) the detection range for IMRIs into Schwarzschild black holes with the same mass. For low spins  $\chi \lesssim 0.4$ , which are typical for intermediate-mass black holes of  $\sim 100 - 200$  solar masses that gained a significant fraction of their mass via minor mergers, we can approximate the detection range increase due to the inclusion of central black hole spin as

$$\frac{\text{Range}_{\text{spin}}}{\text{Range}_{\text{no-spin}}} \sim 1 + 0.6\chi^2 \left( \frac{M}{100 M_{\odot}} \right). \quad (24)$$

This is the ratio of detection ranges; the ratio of detection volumes is a cube of this ratio.

The effects of cosmological redshift are not significant for Advanced-LIGO IMRIs when the black-hole spin is small. Even prograde equatorial inspirals of neutron stars into  $M = 100 M_{\odot}$  black holes spinning at  $\chi = 0.9$  are only detectable to  $z \approx 0.2$  at an SNR threshold of 8. The cosmological redshift has the same effect as increasing the black-hole mass, so including redshift increases the ratio of detection volumes at higher spins. For the purposes of including redshift in Fig. 3, the inspiraling object mass was set to  $m = 1.4 M_{\odot}$  and a detection threshold of  $\text{SNR} = 8$  was assumed.

The results described here do not include higher-order ( $m \neq 2$ ) harmonics of the orbital frequency. Higher harmonics are not significant when black-hole spins are small, since in that case they affect both the spinning and the non-spinning rates roughly equally, and so the ratio does not change. However, for high values of spin, the ratios would probably drop somewhat relative to those given in Fig. 3, since including higher-frequency harmonics would contribute more to increasing the detection range for inspirals into non-spinning holes than into rapidly holes with prograde orbits (cf. Fig. 6 of (Mandel et al. 2007)).

We also compute the dependence of the LISA EMRI detection range on the massive black hole spin. We consider EMRIs of  $m = 10 M_{\odot}$  objects into  $M = 10^5 M_{\odot}$ ,  $M = 10^6 M_{\odot}$ , and  $M = 10^7 M_{\odot}$  massive black holes. We assume that a detection is possible at an SNR threshold of 30. (Setting the threshold to 15 changes the results at the 10 – 20% level.) Cosmological redshift must be included for LISA EMRIs since they can be seen to  $z \sim 1 - 2$ . This means we must specify the inspiraling object mass and the SNR detection threshold, since these are necessary to determine the cosmological redshift of the most distant detectable source.

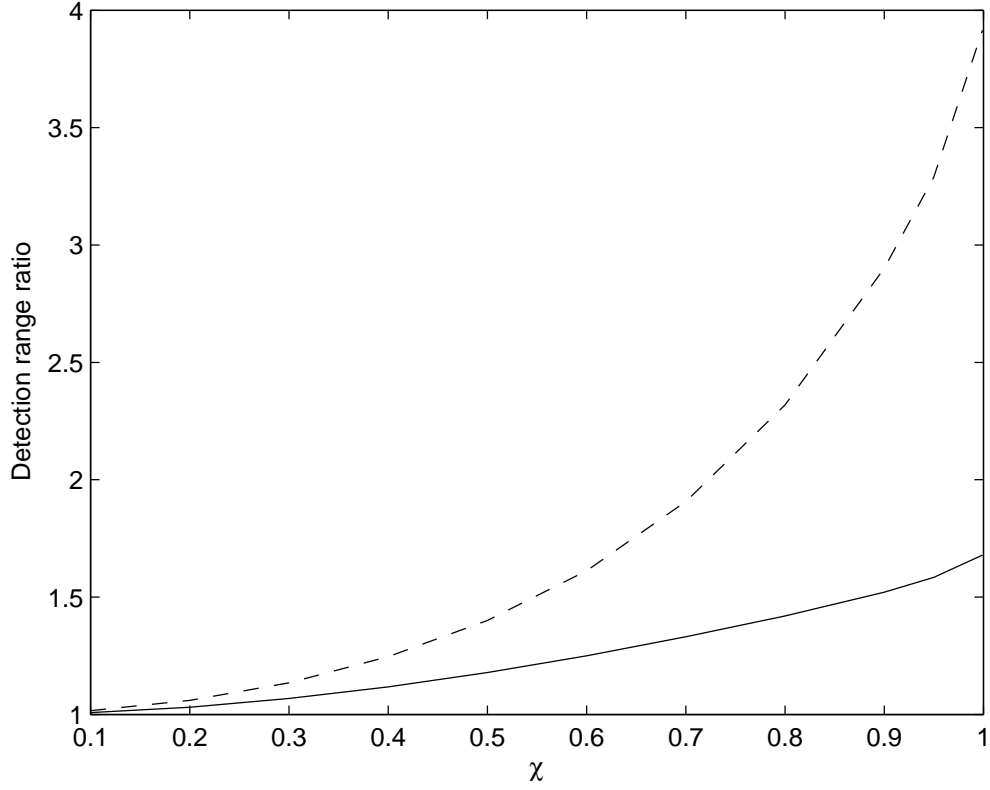


Fig. 3.— The ratio between the inclination-averaged Advanced-LIGO detection range for intermediate-mass-ratio inspirals into Kerr black holes of a given spin and the detection range for IMRIs into non-spinning black holes. The solid curve represents black holes with mass  $M = 100 M_{\odot}$ ; the dashed curve, mass  $M = 200 M_{\odot}$ .

LISA EMRIs only sweep through a fraction of the frequency band during the observation time. Therefore,  $f_{\min}$  for LISA is set not by the detector threshold, but by the frequency of the gravitational waves emitted one year before plunge. We compute  $f_{\min}$  by evolving the gravitational-wave frequency back in time from plunge for one year using the prescription of Barack & Cutler (2004) (Eqs. (28) and (29)).

For  $M = 10^5 M_\odot$ , the spin of the black hole is almost irrelevant: once we average over orbital inclinations, the spin affects the detection range at a level of at most a few percent. This is because at these low masses, most of the SNR comes from the portion of the inspiral at much higher radii than the LSO, so the exact frequency of the LSO does not play a very significant role (cf. Fig. 8 and associated discussion in (Amaro-Seoane et al. 2007)).

Figure 4 shows the dependence of the average EMRI detection range on the massive-black-hole spin for  $M = 10^6 M_\odot$ . The average detection range for EMRIs into rapidly spinning black holes of mass  $M = 10^6 M_\odot$  is  $\sim 13\%$  larger than for EMRIs into non-spinning black holes. For  $M = 10^7 M_\odot$ , the detection range for EMRIs into rapidly spinning black holes is increased by a factor of  $\sim 25$  over those into non-spinning black holes, as shown in Fig. 5. This greater sensitivity to black hole spin is expected, since for these massive black holes most of the SNR comes from the cycles near the LSO. However, this should not be taken to mean that inspirals into rapidly spinning  $M = 10^7 M_\odot$  black holes are likely to dominate LISA EMRI observations. Figures 4 and 5 show detection range ratios only; the inclination-averaged detection range for an EMRI into a maximally spinning  $M = 10^7 M_\odot$  black hole is actually less than the detection range for an EMRI into a non-spinning  $M = 10^6 M_\odot$  black hole. On the other hand, this large ratio does mean that there is a strong detection bias in favor of rapidly spinning black holes, which must be taken into account when statistics of EMRI observations are inverted to gather information about the massive-black-hole spin distribution.

I thank Kip Thorne and Curt Cutler for suggesting this problem, and Luc Bouten, Jonathan Gair and Cole Miller for helpful discussions, and Kip Thorne for thorough comments on the manuscript. I was partially supported by NSF Grant PHY-0099568, NASA Grant NAG5-12834, and the Brinson Foundation.

## REFERENCES

- Barack, L. & Cutler, C. 2004, Phys. Rev. **D69**, 082005
- Fritschel, P. 2003, arXiv:gr-qc/0308090

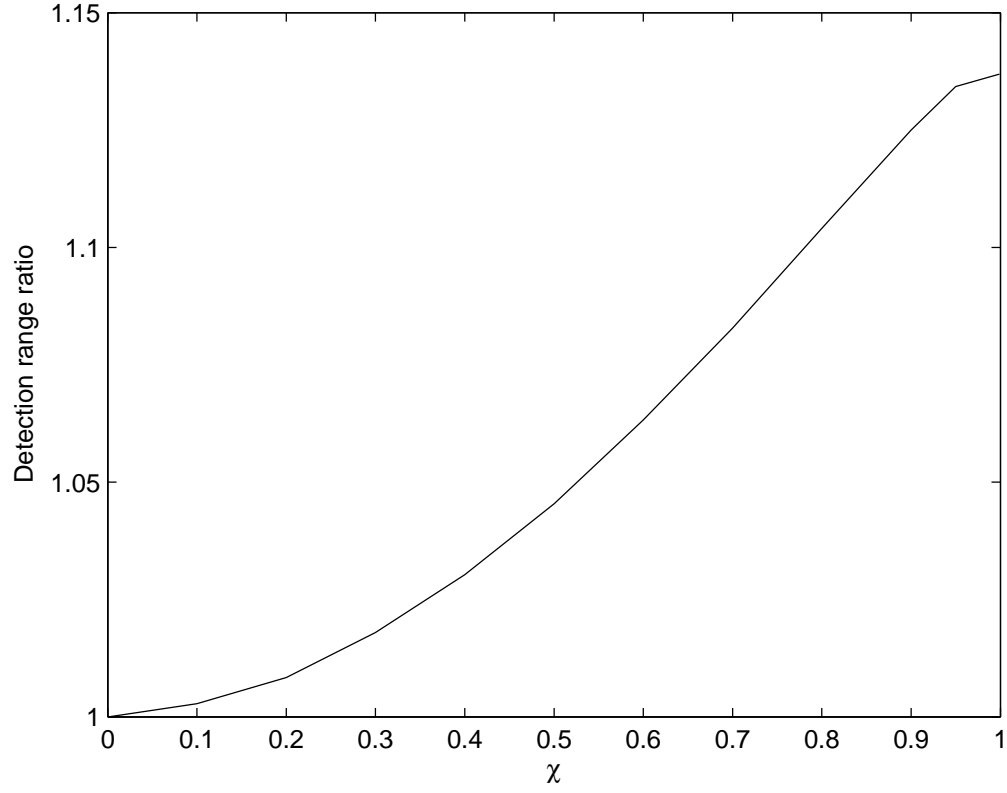


Fig. 4.— The ratio between LISA detection ranges (at SNR= 30) for extreme-mass-ratio inspirals of  $m = 10 M_{\odot}$  compact objects into Kerr black holes of mass  $M = 10^6 M_{\odot}$  and a given spin vs. non-spinning black holes.



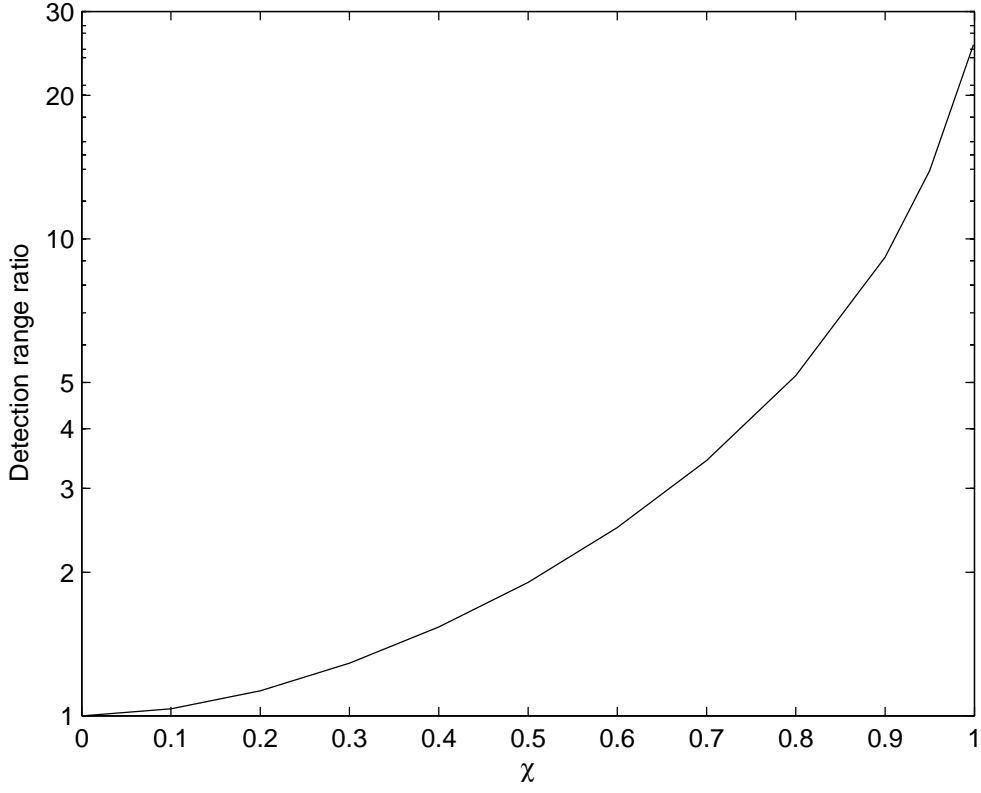


Fig. 5.— The ratio between LISA detection ranges (at SNR= 30) for extreme-mass-ratio inspirals of  $m = 10 M_{\odot}$  compact objects into Kerr black holes of mass  $M = 10^7 M_{\odot}$  and a given spin vs. non-spinning black holes.

- Gültekin, K., Miller, M. C., & Hamilton, D. P. 2004, *ApJ*, 616, 221
- Gültekin, K., Miller, M. C., & Hamilton, D. P. 2006, *ApJ*, 640, 156
- Hughes, S. A. 2000, *Phys. Rev. D* **61**, 084004
- Hughes, S. A. & Blandford, R. D. 2004, *ApJ*, 585, L101
- Mandel, I., Brown, D. A., Gair, J. R., Miller, M. C. 2007, submitted to *ApJ*, arXiv:0705.0285
- Miller, M. C. 2002, *ApJ*, 581, 438
- Miller, M. C., & Colbert, E. J. M. 2004, *IJMPD*, 13, 1
- Miller, M. C., & Hamilton, D. P. 2002a, *MNRAS*, 330, 232
- Miller, M. C., & Hamilton, D. P. 2002b, *ApJ*, 576, 894
- Misner, C. W., Thorne, K. S., & Wheeler, J. A. *Gravitation* (Freeman, San Francisco, 1973)
- Mouri, H., & Taniguchi, Y. 2002a, *ApJ*, 566, L17
- Mouri, H., & Taniguchi, Y. 2002b, *ApJ*, 580, 844
- O’Leary, R. M., Rasio, F. A., Fregeau, J. M., Ivanova, N., & O’Shaughnessy, R. 2006, *ApJ*, 637, 937
- Amaro-Seoane, P., Gair, J. R., Freitag, M., Miller, M. C., Mandel, I., Cutler, C. J., Babak, S. 2007, submitted to *CQG*, arXiv:astro-ph/0703495
- Taniguchi, Y., Shioya, Y., Tsuru, T. G., & Ikeuchi, S. 2000, *PASJ*, 52, 533